Modified Kirchhoff prestack depth migration using the Gaussian Beam operator as Green function – Theoretical and numerical results

C. A. S. Ferreira and J. C. R. Cruz

email: *casf@ufpa.br*

keywords: *Kirchhoff migration, Gaussian Beam, Green function*

ABSTRACT

The Gaussian Beam concept has been of great importance for works on modeling and migration, during the last two decades. This work then joins the flexibility of the true amplitude (diffraction stack) Kirchhoff migration procedure with the regularity description of the wavefield represented by the Gaussian Beam. We apply our final operator in some simple numerical examples of geophysical exploration interest. Our process can be named as Kirchhoff Gaussian Beam Prestack Depth Migration (KGB-PSDM) in a true amplitude sense.

INTRODUCTION

In the last two decades, Kirchhoff migration has evolved from a kinematic, imaging only technique, to an inversion operator capable of handling important informations to AVO/AVA analysis. Bleistein (1987), based on Beylkin (1985), was one of the first researchers to propose an inversion algorithm that used the Kirchhoff algorithm to determine seismic attributes from migrated data, such as the (angle-dependent) reflection coefficients along reflectors. Later, Schleicher et al. (1993), based on Hubral et al. (1991), developed a 3D, true amplitude, finite-offset, migration formalism that performed the role of imaging and inversion for different acquisiton geometries, freeing seismic data from its geometrical spreading losses.

Although of all the developments reached so far by these techniques, the migration algorithms described above still make an extensive use of the (zero order) ray theory to simulate the Green's function of the imaging problem. In seismic methods, ray theory plays an important role in modeling, imaging and inversion. However, ray theory can only be effectively applied to smooth media, where the characteristic wavelenght of the seismic energy is much smaller than the structural dimensions we want to image. In this case, some wavefield phenomena in complex geology media, such as diffractions, cannot be adequately simulated. In such a situation, structures such as dome flanks and some other discontinuities, such as faults, cannot be properly imaged. Ray theory simply fails in these cases, since the ray code does not lead with inhomogeneous waves.

The paraxial ray theory has been an attractive and efficient way of dealing with the drawbacks of the ray theory (Červený, 1983). In general, these wavefields are of real and complex nature. The real paraxial theory is widely applied in the field of classical optics, while the complex paraxial theory is widely used in quantum optics, where the Gaussian beams are well known quantities in laser propagation. In seismic imaging, the real paraxial theory has been widely applied in stacking methods, such as CRS (Common Reflection Surface), while the complex paraxial theory (Guassian Beams or simply GB's) has been applied to simulate 2D and 3D laterally varying wavefields (Popov, 1996; Červený, 1982; Červený et al., 1982), as well as in migration methods (Hill, 2001).

One of the main advantages of the complex paraxial theory approach is related to its regularity in the description of the wavefield in singular regions of the velocity model, and the lack of necessity of using one subroutine called two point raytracing. Particularly, the GB's are regular even in regions where caustics predominates, where the ray tubes shrink to points or lines and give rise to a phase shift change in

amplitudes. Besides that, bearing in mind that two point ray tracing is not necessary, the paraxial theory can be used to simulate wavefields in irregular regions of the model, where a ray cannot be traced (shadow zones).

In this work, we make use of GB's (Popov, 1996; Červený, 2001) to perform a 3D prestack depth migration based on the formalism of Schleicher et al. (1993). By introducing the GB superposition integral into the kernel of the (diffraction stack) migration integral and making use of the Fresnel volume elements (Schleicher et al., 1997; Schleicher et al., 2004), the inner integral is reinterpreted as having its integration domain projected towards the acquisition surface, along the projected Fresnel zone of each trace, and whose weight-function is proportional to the same quantity. In the data domain, this means that each trace is influenced also by reflector properties that are included in neighbour traces, which now are stacked in order to enhance the horizontal resolution of the migrated data. It is well known that in the vicinity of points in depth, over reflector surfaces, the seismic wavefield is smeared during reflections, and that the knowledge of this smearing region influences in the migration aperture choice (Schlicher et al., 1997). Our final GB operator, then, explicitly uses this information before the diffraction stacking, inserting again in each trace to be staked the neighbour information smeared during the wavefield propagation.

MODIFIED KIRCHHOFF INTEGRAL

Our starting point is the migration integral described in Schleicher et al. (1993), here defined in the frequency domain

$$\hat{V}(\boldsymbol{M},\omega) = -\frac{i\omega}{2\pi}\int_A d\xi_1\, d\xi_2\, w(\vec{\xi},\boldsymbol{M})\, U(\vec{\xi},\omega)\, e^{i\,\omega\tau_D(\vec{\xi},M)}, \tag{1}$$

where A is the migration aperture, $M = M(x,y)$ represents a point in depth, $w(\vec{\xi},\boldsymbol{M})$ is a weight function that corrects seismic amplitudes from its geometrical spreading losses, $\vec{\xi} = (\xi_1,\xi_2)^T$ is a coordinate vector along the acquisition surface, $\tau_D(\vec{\xi},\boldsymbol{M})$ is the diffraction (Huygens) surface, and $U(\vec{\xi},\omega)$ is the analytical particle displacement, which is formed by the real displacement $u(\vec{\xi},\omega)$ plus its Hilbert transform as imaginary part. In the present case, we consider that the primary reflections from the reflectors we want to image, described for each source-receiver pair (S,G), are distributed along a reflection surface $\tau_R(\vec{\xi})$.

In our current derivation, attention must be paid to factors $w(\vec{\xi},M)$, $U(\vec{\xi},\omega)$ and $\tau_R(\vec{\xi})$. The adjustment of $w(\vec{\xi},M)$ to several acquisition geometries, considering elements of paraxial ray theory, grants that reflection amplitudes are corrected dealt in the migration process (Schleicher et al., 1993). Thus, for convenience, we must guarantee that our approach yields in the same situation. As for the reflection traveltime $\tau_R(\vec{\xi})$, in dealing with GB's the amplitudes are Gaussian decaying with respect to the distance from the central ray (Červený, 2001), and here this is done so by considering that traveltimes are complex valued functions, its imaginary part representing the so called GB's half-width (Popov, 1996; Červený, 2001). Finally, let us consider that $U(\vec{\xi},\omega)$ is the Green function of our imaging problem and that it is represented by a superposition of GB's (Ferreira & Cruz, 2004 a,b)

$$U(\vec{\xi},\omega) = \int_{A_P} d\xi_1^P d\xi_2^P\, \frac{det\boldsymbol{\Lambda}}{det\mathbf{H}_F}\, \frac{det\mathbf{Q}(\vec{\xi}^P)}{\cos\theta_G}\, \Phi(\vec{\xi}^P)\, A(\vec{\xi}^P)\, e^{-i\omega\tau_R(\vec{\xi},\vec{\xi}^P)}, \tag{2}$$

where $\mathbf{H}_F$ is the Fresnel zone matrix and $\boldsymbol{\Lambda} = \boldsymbol{\Gamma}_S^T\,\mathbf{N}_{SR} + \boldsymbol{\Gamma}_G^T\,\mathbf{N}_{GR}^T$, where $\mathbf{N}_{SR}$ and $\mathbf{N}_{RG}$ are traveltime second time derivatives 2 x 2 matrices defined in Schleicher et al. (1993), while $\boldsymbol{\Gamma}_S^T$ and $\boldsymbol{\Gamma}_G^T$ are 2 x 2 matrices related to the acquisition geometry. Coordinates $\vec{\xi}^P = (\xi_1^P,\xi_2^P)$ belong to a subset of the migration aperture A, corresponding to the projected Fresnel zone, here denominated A_P. We will consider in this work that this subaperture is restricted only to the first projeted Fresnel zone. $det\mathbf{Q}(\vec{\xi}^P)$ and $\cos\theta_G$ are quantities related to the geometrical spreading and to the incidence angle at G (geophone), respectivelly. This integral representation of the GB's was obtained by considering that the endpoints of the rays, parameterized by ray parameters $\gamma = (\gamma_1,\gamma_2)$, strike an artbitrary surface (fictitious or not) along the raypath and form a set of points that give rise to a region around the reflection point M_R, known as Fresnel zone (Schleicher et al., 2004). By using Bortfeld's surface-to-surface propagator (Bortfeld, 1989; Schleicher et al., 2004), we assign a linear relationship among points belonging to the Fresnel zone in depth and its projected counterpart, along the aquisition surface. This relationship works, in this case, as

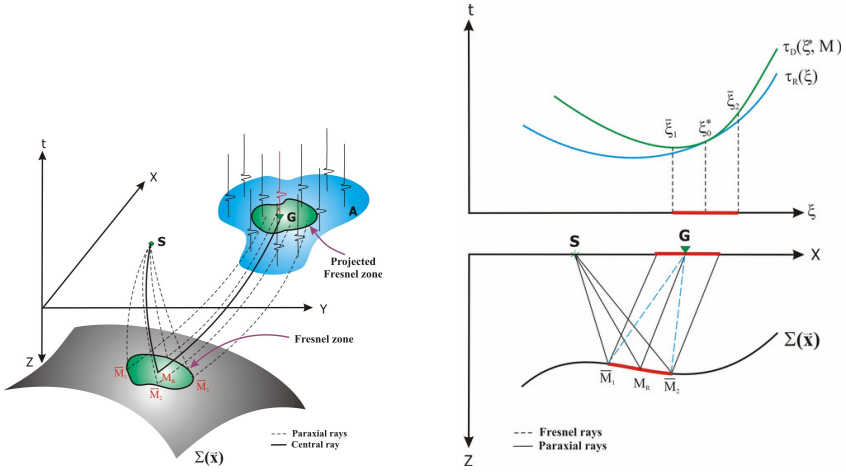

Figure 1: (a) Fresnel zone in depth and its projection towards the acquisition surface. (b) Specular ray SM_RG, its Fresnel zone in depth, the paraxial rays and the projected Fresnel zone. Point $\vec{\xi}_0^*$ is a stationary point belonging to the Huygens surface. The (paraxial) points $\vec{\xi}_1$ and $\vec{\xi}_2$ also belong to the reflection curve.

a transformation Jacobian, and permits that we define a region of integration for the GB's along the Earth surface, and more especifically along the projected Fresnel zone, whose position-vector is represented by $\vec{\xi}^P$. The weight-function $\Phi(\vec{\xi}^P)$ is a quantity that asymptotically reduces Eq. (2) to the zero order ray theory solution (Červený, 2000). In this work, it is represented by (Ferreira & Cruz, 2004 a,b)

$$\Phi(\vec{\xi}^P) = \frac{i\omega}{2\pi}\sqrt{det\mathbf{H}_F(\vec{\xi}^P)}\,(det\mathbf{Q}(\vec{\xi}^P))^{-1}\,\cos\theta_G. \tag{3}$$

Finally, $A(\vec{\xi}^P)\,e^{-i\omega\tau_R(\vec{\xi},\vec{\xi}^P)}$ represents the paraxial contribution at positions $\vec{\xi}^P$ that influences the observations at $\vec{\xi}$, where $\tau_R(\vec{\xi},\vec{\xi}^P)$ is the complex traveltime in $\vec{\xi}$ due to an event observed in $\vec{\xi}^P$. The fact that Eq. (3) is proportional to the Fresnel zone is in agreement with the fact that when GB's propagate through a medium and are reflected in a specific reflecting surface, it "illuminates" a region around a central ray, where all paraxial rays are concentrated, i.e., where energy is flowing alongside (Figure 1a). In this way, we introduce a physical significance to the weight function asymptotically derived by Klimeš (1984) and Červený (2000). It simply "weighs" the events belonging only to the first Fresnel zone, disregarding other events belonging to several other zones.

Now let us introduce expression (3) and (2) into Eq. (1) and analyse the physical significance of the resulting integral. After eliminating all the symmetrical terms, we have

$$\hat{V}(M,\omega) = (\frac{\omega}{2\pi})^2 \int_A d\xi_1\,d\xi_2\,w(\vec{\xi},M)\int_{A^P} d\xi_1^P\,d\xi_2^P\,\sqrt{det\,\mathbf{H}_P}\,A(\vec{\xi}^P)\,e^{[i\omega(\tau_D(\vec{\xi},M)-\tau_R(\vec{\xi},\vec{\xi}^P))]}. \tag{4}$$

Back to the time domain, this equation becomes

$$V(M,t) = \frac{1}{4\pi^2}\int_A d\xi_1\,d\xi_2\,w(\vec{\xi},M)\int_{A^P} d\xi_1^P\,d\xi_2^P\,\sqrt{det\,\mathbf{H}_P}\,\ddot{U}[\vec{\xi},t\,+\,\tau_D(\vec{\xi},M)]. \tag{5}$$

The factor $\ddot{U}$ is the second time derivative of the analytical particle displacement, while A and A_P are the migration and the projected Fresnel zone apertures, respectively.

In Figure 1b we have a detailed geometrical interpretation of Eq. (5). In 2D, we see a seismic experiment where a specular ray SM_RG and the Fresnel (paraxial) rays SM_jG ($j = 1, 2, \ldots, n$) determine the

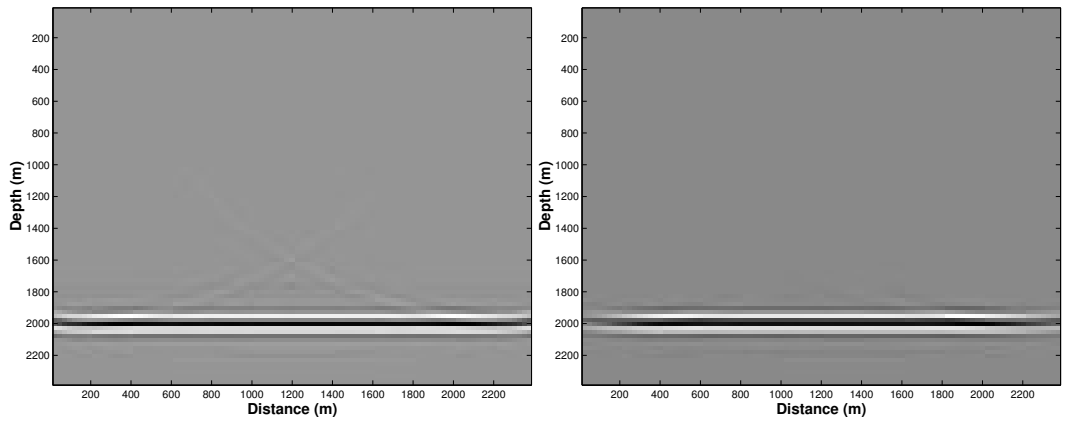

(a) **(b)**

Figure 2: (a) Kirchhoff PSDM for the horizontal plane reflector. (b) KGB-PSDM migration for the same reflector. Note that migration artifacts on the borders were automatically eliminated by the process.

formation of a Fresnel zone in depth and its subsequent projection towards the acquisition surface. According to the diffraction stack theory (Schleicher et al., 1993), point $\vec{\xi}_0^*$ is a stationary point corresponding to a reflection event in M_R, which in turn belongs to a diffraction curve exactly where there exists a tangency with the reflection curve. With the determination of the projected Fresnel zone along the acquisition surface for the reference trace $\vec{\xi}_0^*$, we can find points $\overrightarrow{\xi_j}$, which belongs to this zone, and that are part of the same reflection surface corresponding to points in the vicinity of M_R in depth, and stack them with the help of the inner integral in (5). These projected events, which are contained in the reflection traveltime surface $\tau_R(\vec{\xi})$, serve as input for the diffraction traveltime surface $\tau_D(\vec{\xi}, M)$, which are stacked a posteriori by the outer integral in (5).

SYNTHETIC EXAMPLES

We have implemented Eq. (5) for the imaging of geological models composed of plane reflectors and curved reflectors, inserted in an homogeneous medium with layers of constant velocity. We consider that the models are composed of one single reflector, above which we consider P waves with propagation velocity $v_1 = 2.0Km/s$, and below it we consider propagation velocities $v_2 = 3.5Km/s$. In order to acquire synthetic data for the migration process, we have performed a 2.5D Kirchhoff modeling scheme, using a common offset acquisition geometry, with $2h = 25m$ in the first case, and $2h = 15m$, in the second case. In the case of the plane reflectors, the spacing among sources and geophones is $25m$, while for the curved reflectors we have considered spacings among sources and geophones of $15m$. For both cases, we have used a zero phase Gabor wavelet, with total durations of $50ms$ and $20ms$, and dominant frequencies of $10Hz$ and $20Hz$, respectively. In the migration procedure, the 2.5D GB (Green function) is a 2D version of the inner integral in Eq. (2), only considering that in-plane factors were taken in consideration in order to adequately simulate the amplitudes.

In the cases studied below, the Fresnel volume elements (in depth or projected along the acquisition surface) were completed determined using dynamic raytracing (DRT) (Červený, 2001). More especifically, complex initial conditions for the DRT were chosen in order to generate quantities related to the GB's itself (i.e., beam half-width, wavefront curvature, etc.). In order to guarantee GB's with minimum half-widths at the geophones, we have used plane waves initial conditions, using the criteria described by Müller (1984). Since the synthetic data are not the main objective of our studies, only the imaging results will be shown in the following.

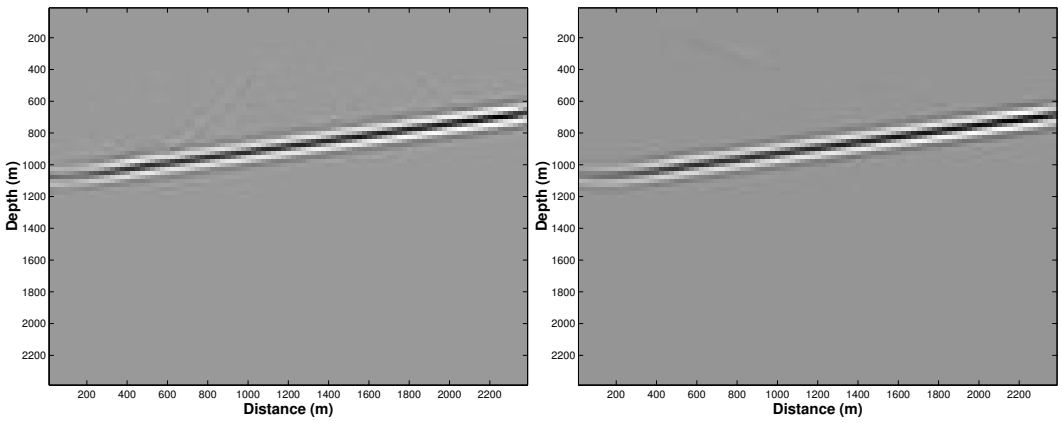

(a) **(b)**

Figure 3: (a) Kirchhoff PSDM for the plane dipping reflector. (b) KGB-PSDM migration for the dipping reflector.

Plane reflectors

In this first example, we consider two plane reflectors, the first one is horizontal, located at depth $z = 2km$, while the second reflector dips 7^0 to the left, beginning with a depth of $z = 1.1km$, on the left, and ending with a depth of $z = 0.7km$, on the right. In these examples, we have used a grid spacing for the migration procedures of $\Delta x = \Delta z = 25m$.

In Figure 2a, we have the result of the conventional Kirchhoff PSDM, where the reflector was reconstructed in its true subsurface position. As it is well known, migration artifacts appear on the borders of the image, due to insufficient data to stack (Hertweck et al., 2003). KGB-PSDM, which considers the stacking of all traces belonging to the projected Fresnel zone (Figure 2b), automatically eliminates these artifacts. The latter image, in general, is cleaner than the one obtained by the conventional Kirchhoff procedure.

In the case of the dipping reflector (Figures 3a and 3b), the image of the structure is again reconstructed in its true subsurface position and we have the same effects as depicted in Figure 2. The right and left artifacts are not seen in the KGB-PSDM image, as they are seen in Kirchhoff PSDM, but in this case "some" artifact, almost invisible, seems to be produced near depths $200 - 400m$. Overall, the KGB-PSDM image is again less aliased than the image produced by Kirchhoff PSDM.

As for the amplitudes, in both images there seems to be some differences with respect to each reflector in consideration. In the horizontal reflector case, amplitudes seem to behave well along the whole reflector, but near the borders the resolution seems to be reduced. This fact may be related to the influence of the number of traces inside the projected Fresnel zones, since we can only account, on both borders, with half the number of taces belonging to the projected zones at these locations. On the other hand, in the case of the dipping reflector this fact does not seem to influence the final result. Either on the right border or on the left border the amplitudes reconstructed by the KGB-PSDM process seem to be the same as in the case of Kirchhoff PSDM.

In Figures 4 we have made comparisons of the picked peak amplitudes for the horizontal and dipping reflectors, respectively. In the case of the horizontal reflector (Figure 4a), we observe an agreement in amplitude trends, but the KGB-PSDM overestimates amplitudes by, at least, 3% more the amplitudes along the whole reflector, far from the borders. This is related to the stacking of more information to each point in depth due to its contributing vicinity. On the borders itself, there occurs an underestimation of amplitudes, as we have previously noticed. But even so, the agreement in the trend is excellent. For the dipping reflector (Figure 4b), the situation that apparently seemed better than in the case of the horizontal reflector shows an initial underestimation on the left border, followed by an agreement upward and an overestimation on the

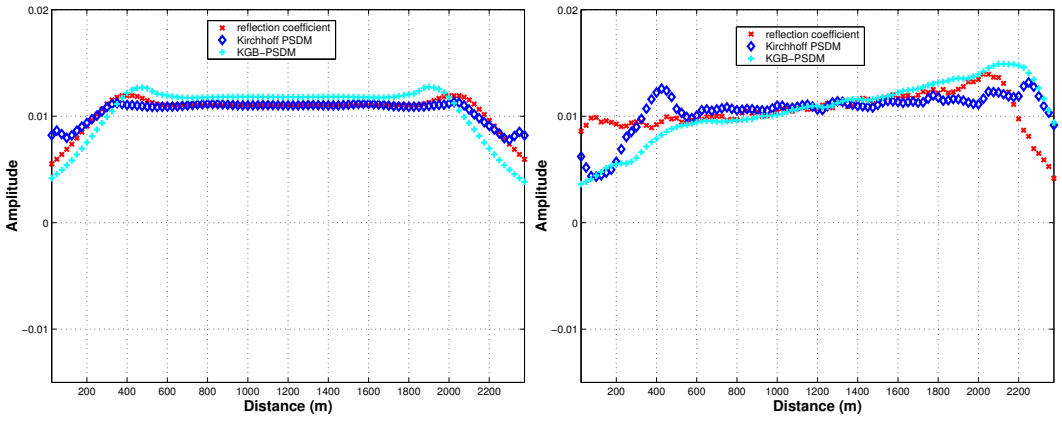

(a) **(b)**

Figure 4: (a) Comparison of amplitudes for the horizontal refletor. (b) Comparison of amplitudes for the dipping reflector.

right border. The trend in amplitudes, however, is in excellent agreement.

Curved reflectors – syncline model

In this example we consider the existence of a curved reflector in the form of a syncline, the borders of it located at depth $z = 0.8km$, while its trough reaches a depth of $z = 1.1km$. We have used as discretization grid for the migration process the values $\Delta x = \Delta z = 15m$. In Figure 5a we have the result of the Kirchhoff PSDM for the syncline reflector. Again border effects inherents to the migration process are observed at these places due to insufficient data to stack. Figure 5b, then, shows the results of the KGB-PSDM procedure on the same model. Visually we note a decrease of the border effects and some higher quality in the final image resolution.

For a quantitative measure, in Figure 6 we show a comparison of the recovered amplitudes using the two migration procedures, where the picked peak amplitudes were taken along the reflectors. We must call attention to the fact that in this case we have not compared both methods with respect to the amplitudes calculated using the 2.5D Kirchhoff modeling scheme. This was not possible due to the fact that the syncline model presents more than one single arrival in some receivers located in the caustic region. In this specific case, we have up to three arrivals for the same receiver in its caustic regions (trough region of the syncline), and this force us to separate each arrival in order to compare the amplitude recovering (Tygel et al., 1998). In this way, we have chosen only to compare the two methods of amplitude recovering. This is exactly what is depicted in Figure 6. We then observe a excellent agreement in the trends of the curves, of course with some isolated particularities. Generally speaking, the KGB-PSDM procedure is equivalent to the Kirchhoff PSDM along the whole reflector. On the left, we observe a small overestimation in amplitudes, but with an excellent trend in the behaviour of the amplitudes. On the rest of the reflector, the behaviour of the amplitude curves for the KGB-PSDM procedure estimates in excellent agreement the amplitude values, but on the left border there occurs an underestimation in the amplitude values. Again, the agreement in the amplitude trends is excellent when compared to the traditional method.

ALGORITHM

In order to summarize what we have done so far, in the following we list the five main steps (S's) in obtaining our true amplitude KGB-PSDM migration:

S1 – An arbitrary depth point M is chosen and its ray, amplitude, and traveltime towards position $\vec{\xi}$ are

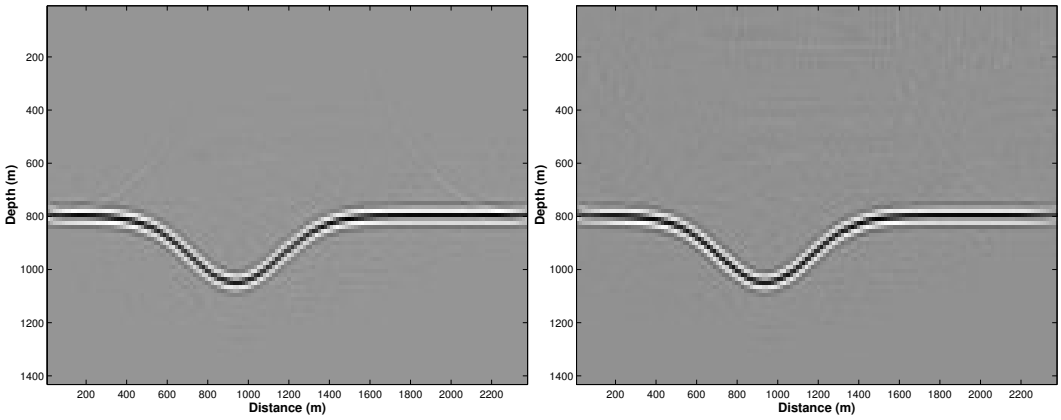

(a) **(b)**

Figure 5: (a) Kirchhoff PSDM for the syncline reflector. (b) KGB-PSDM migration for the syncline reflector.

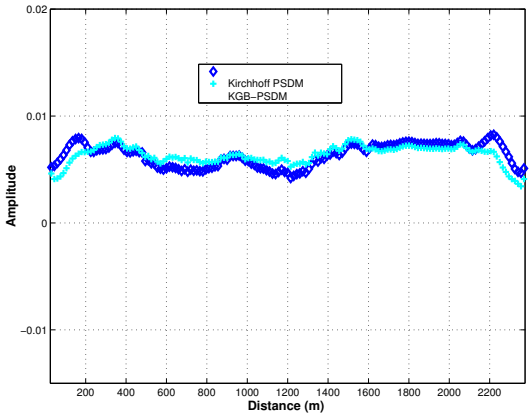

Figure 6: Picked peak amplitudes comparison between the KGB-PSDM and the Kirchhoff PSDM procedures. No peak amplitudes were taken from the modeled data, due to the presence of multiple arrivals in distinct areas along several receivers in the trough region of the model.

determined, together with its Fresnel volume.

S2 – Computation of the diffraction traveltime surface $\tau_D(\vec{\xi}, M)$.

S3 – Computation of the projected Fresnel zone and beam formation restricted to the projected Fresnel zone, parameterized by position vector $\vec{\xi}^P$.

S4 – Gaussian Beam superposition to obtain the input location for the migration integral, defining the Huygens surface.

S5 – Kirchhoff summation.

CONCLUSIONS

We have developed a prestack Kirchhoff-type depth migration in that we consider as Green function an integral superposition of Gaussian Beams.

We have tested the KGB-PSDM algorithm on plane and curved geological models. In the plane models, we have considered two distinct cases: the first, representing an horizontal interface; and a second, representing a plane interface dipping to the left. Both images were obtained considering an homogeneous medium. In using the KGB-PSDM algorithm for these two examples, the final images obtained have shown a considerable reduction of the migration artifacts, the so called "migration smiles". Some lack of resolution (as in the case of the horizontal reflector) is observed on the borders of both images, due to the insufficient number of traces belonging to the projected Fresnel zones located on the borders of the seismic data, but the overall images are less aliased than the ones produced by a conventional Kirchhoff PSDM.

The picking of peak amplitudes for these two first examples has shown several effects that are not seen on the images. In both cases, the trend of amplitudes is in excellent agreement, but on the borders there occurs overestimation and underestimation of amplitudes. Far from the borders, the KGB-PSDM process seems to overestimates amplitudes by, at least, 3%. This is related to the stacking of all the vicinity points in depth in the image point, thus increasing the values of the amplitudes.

The KGB-PSDM algorithm has also been tested on a curved geological model, represented by a syncline model. While the image obtained by the conventional Kirchhoff procedure showed the expected presence of the migration smiles, the KGB-PSDM procedure recovered a less aliased image and automatically tapered these artifacts on the borders. The comparison of picked peak amplitudes showed a similar behavior as the ones obtained for the plane reflectors, with an excellent agreement in the trends of the curves. For this particular syncline example, we have compared only the amplitude estimation derived from the Kirchhoff PSDM and the KGB-PSDM procedures, respectively, since the syncline model example presents multiple arrivals due to the presence of a caustic zone (buried focus) located on the trough of the structure. In this case, the events belonging to this region should be isolated, according to each arrival, and only in doing so it would be possible to compare the Kirchhoff and KGB-PSDM true amplitude recovering with respect to the true reflection amplitudes along these regions.

ACKNOWLEDGMENTS

The first author thanks the Brazilian National Research Council (CNPq) for the financial support (PhD scholarship) during all the stages of this research.

REFERENCES

Beylkin, G., 1985. Imaging of discontinuities in the inverse scattering formalism by inversion of a generalized Radon transform. J. Math. Phys., **26**, 99-108.

Bleistein, N., 1987. On the imaging of reflectors in the Earth. Geophysics, **52**, 931-942.

Bortfeld, R., 1989. Geometrical ray theory: rays and traveltimes in seismic systems (second-order approximation of the traveltimes). Geophysics, **54**, 342-349.

Červený, V., 1982. Expansion of a plane wave into Gaussian beams. Studia Geoph. et Geod., **26**, 120-131.

Červený, V.; Popov, M. M.; Pšencik, I., 1982. Computations of wavefields in inhomogeneous media – Gaussian beam approach. Geophys. J. R. astr. Soc., **70**, 109-128.

Červený, V., 1983. Synthetic body wave seismograms for laterally varying layered structures by the Gaussian beam method. Geophys. J. R. astr. Soc., **73**, 389-426.

Červený, V., 2000. Summation of paraxial Gaussian beams and of paraxial ray approximations in inhomogeneous anysotropic layered structures. In: Seismic Waves in Complex 3D Structures, Report 10. Charles University, Prague, 121-159.

Červený, V., 2001. Seismic ray theory. Oxford University Press.

Ferreira, C. A. S.; Cruz, J. C. R., 2004. Modified Kirchhoff prestack migration using the Gaussian Beam operator as Green function. EAGE 66th Conference & Exhibition. Paris, France. Expanded abstracts.

Ferreira, C. A. S.; Cruz, J. C. R., 2004. Migração pré-empilhamento em profundidade usando o operador de feixes gaussianos como função de Green – Teoria. I Workshop da Rede Norte de Pesquisa em Risco Exploratório. Natal-RN, Brazil, Expanded abstract.

Hertweck, T.; Jäger, C.; Goertz, A.; Schleicher, J., 2003. Aperture effects in 2.5D Kirchhoff migration: a geometrical explanation. Geophysics, **68**, 1673-1684.

Hill, N. R., 2001. Prestack Gaussian beam depth migration. Geophysics, **66**, 1240-1250.

Hubral, P.; Tygel, M.; Zien, H., 1991. Three dimensional true-amplitude zero-offset migration. Geophysics, **56**, 18-26.

Kliměs, L., 1984. Expansion of a high frequency time harmonic wavefield given on an initial surface into Gaussian beams. Geophys. J. R. astr. Soc., **79**, 105-118.

Müller, G., 1984. Efficient calculation of Gaussian Beam seismograms for two-dimensional inhomogeneous media. Geophys. J. R. astr. Soc., **79**, 153-166.

Popov, M. M., 1996. Ray theory and Gaussian beam method for geophysicists. PPPG, UFBA, 148p.

Schleicher, J.; Tygel, M.; Hubral, P., 1993. 3D true-amplitude finite-offset migration. Geophysics, **58**, 1112-1126.

Schleicher J.; Hubral, P.; Tygel, M.; Jaya, M. S., 1997. Minimum apertures and Fresnel zones in migration and demigration. Geophysics, **62**, 183-194.

Schleicher, J.; Tygel, M.; Hubral, P., 2004. True-amplitude seismic imaging. Monografia, Society of Exploration Geophysicists. Submitted.

Tygel, M.; Schleicher, J.; Hubral, P.; Santos, L. T., 1998. 2.5D true-amplitude Kirchhoff migration to zero-offset in laterally inhomogeneous media. Geophysics, **63**, 557-573.